Received: 2 May 2017 | Accepted: 29 June 2017

DOI: 10.1111/jace.15065

ORIGINAL ARTICLE

Journal of the American Ceramic Society

Controlling phase separation of $Ta_xHf_{1-x}C$ solid solution nanopowders during carbothermal reduction synthesis

Paniz Foroughi[1,2] | **Cheng Zhang**[1] | **Arvind Agarwal**[1] | **Zhe Cheng**[1,2]

[1]Department of Mechanical and Materials Engineering, Florida International University, Miami, Florida

[2]Center for the Study of Matter at Extreme Conditions (CeSMEC), Florida International University, Miami, Florida

Correspondence
Zhe Cheng, Department of Mechanical and Materials Engineering, Florida International University, Miami, FL.
Email: Zhcheng@fiu.edu

Abstract

Synthesis of single-phase tantalum hafnium carbide ($Ta_xHf_{1-x}C$, $0<x<1$) solid solution nanopowders via carbothermal reduction (CTR) reaction is complicated due to the difference in reactivity of parent oxides with carbon and presence of a miscibility gap in TaC-HfC phase diagram below ~887°C. These can lead to phase separation, ie, formation of two distinct carbides instead of a single-phase solid solution. In this study, nanocrystalline $Ta_xHf_{1-x}C$ powders were synthesized via CTR of finely mixed amorphous tantalum-hafnium oxide(s) and carbon obtained from a low-cost aqueous solution processing of tantalum pentachloride, hafnium tetrachloride, and sucrose. Particular emphasis was given to investigate the influences of starting compositions and processing conditions on phase separation during the formation of carbide phase(s). It was found that due to the immiscibility of Ta-Hf oxides and relatively fast CTR reaction, individual nano-HfC and TaC phases form quickly (within minutes at 1600°C), then go through interdiffusion forming carbide solid solution phase. Moreover, the presence of excess carbon in the CTR product slows down the interdiffusion of Ta and Hf dramatically and delays the solid solution formation, whereas DC electrical field (applied through the use of a spark plasma sintering system) accelerates interdiffusion significantly but leads to more grain growth.

KEYWORDS

nanomaterials, phase separation, solid solutions, tantalum/tantalum compounds, ultrahigh-temperature ceramics

1 | INTRODUCTION

Among all ultrahigh-temperature ceramics (UHTCs), hafnium carbide (HfC, T_m=3900°C) and tantalum carbide (TaC, T_m=3880°C) are of particular interest due to their extremely high melting points, high hardness (TaC: ~19 GPa and HfC: ~20 GPa), and high electrical and thermal conductivity and are promising candidates for many important applications that may need to tolerate temperatures above 2000°C.[1-5] Previous studies show that by tailoring the composition (eg, via using alloying elements), ternary UHTC solid solutions and related composites could provide even better properties than simple binary UHTCs, such as further improved oxidation resistance and/or mechanical properties.[6-10] In addition to optimizing the composition, reducing the particle size of these materials from micrometer to submicrometer or nanometer range (~100 nm) provides additional benefits in terms of simplified postsynthesis processing and improved mechanical properties.[1,11,12] All these motivate the research on the synthesis of nanoscale $Ta_xHf_{1-x}C$ ($0<x<1$) ternary solid solution and related composite powders.

Although the synthesis of $Ta_xHf_{1-x}C$ solid solution/composite powders has been studied for some time, the methods reported in the literature all suffer from some drawbacks, such as high cost, inferior product quality and/

or concerns with process safety.[10,13,14] In addition, it is noted that all powder syntheses reported in the literature are performed on a single, Ta-rich composition of $Ta_{0.8}Hf_{0.2}C$, whereas there is no study on the synthesis of Hf richer compositions such as $Ta_{0.5}Hf_{0.5}C$, which sometimes shows even better mechanical properties[15] and oxidation resistance.[16] Because of these, there is a need for better synthesis methods to produce nanocrystalline $Ta_{1-x}Hf_xC$ powders, especially for those with alternative compositions.

However, examination of the TaC-HfC system suggests some challenges regarding controlling the exact phase(s) that would be obtained: The TaC-HfC phase diagram available shows that the two individual carbides would form a continuous solid solution at high temperature.[17] However, there is also a wide miscibility gap with critical temperatures of ~887°C, which suggests that at a lower temperature a TaC-HfC two-phase composite would be energetically more stable than the uniform solid solution over a large composition range for $Ta_xHf_{1-x}C$ (e.g., at room temperature x is between ~0.05 and ~0.98). This means uniform, single-phase $Ta_xHf_{1-x}C$ solid solution powder, even after it is formed at a higher temperature, would have a tendency to go through phase separation under certain conditions such as slow cooling to room temperature. Because solid solution and related two-phase composite often offer different properties,[18] understanding when and how the phase separation would occur and learning to control it during the synthesis of $Ta_xHf_{1-x}C$ nanopowders is expected to bring significant new insights to the general field of nanoscience and engineering and help understand other related systems.[19,20]

In this study, the authors report a low-cost synthesis method to produce nanosized $Ta_xHf_{1-x}C$ solid solution and related nanocomposite powders through aqueous solution-based processing starting from inorganic metal salts of tantalum pentachloride ($TaCl_5$) and hafnium tetrachloride ($HfCl_4$) and soluble hydrocarbon (eg, sucrose) as the metal and carbon precursors, respectively. The simple equipment and cost-effectiveness of the CTR reaction are preserved in this method to convert the metal and carbon precursors into metal carbide(s). In addition, the precursors and processing conditions could also be easily modified for CTR reaction, which enables better control of product morphology, composition, and phase. For the current system, the initial step of solution processing would yield a fine, even nanoscale mixture of Ta-Hf oxide(s) and carbon, which would then go through the CTR reaction in which oxides of tantalum and hafnium are reduced by carbon to form carbide(s), and the overall CTR reaction (assuming formation of a single-phase solid solution) can be written as below:

$$x\mathrm{Ta_2O_5} + 2(1-x)\mathrm{HfO_2} + (6+x)\mathrm{C} = 2\mathrm{Ta_xHf_{1-x}C} + (\mathrm{x}+4)\mathrm{CO} \quad (1)$$

As mentioned before, due to the presence of a miscibility gap in the TaC-HfC system, the ternary $Ta_xHf_{1-x}C$ powder may exist as a uniform solid solution, a nanocomposite of individual carbide phases, or their mixture. Therefore, particular focus was given to revealing the effects of various factors from starting composition to processing conditions on promoting/inhibiting phase separation in the TaC-HfC system, and the fundamental understanding generated is expected to guide synthesizing nanopowders for other multicomponent materials.

2 | EXPERIMENTAL PROCEDURE

For $Ta_xHf_{1-x}C$ powder synthesis, the starting metal precursors used are tantalum pentachloride ($TaCl_5$, 99.8%, Alfa Aesar # 14164) and hafnium tetrachloride ($HfCl_4$, 98+%, Alfa Aesar # 11834). Sucrose (99.5%, SIGMA # S9378) and phenolic resin (Plenco, 14353, R5420) were used as carbon sources for the aqueous and nonaqueous systems, respectively. Totally, five recipes were adopted, as summarized in Table 1. For recipes R6, R7, R11, and R13 that

TABLE 1 Weight ratio of $TaCl_5$, $HfCl_4$ and sucrose ($C_{12}H_{22}O_{11}$) or phenolic resin $(C_6H_6O{\cdot}CH_2O)_x$ and expected Ta:Hf:C molar ratio used in this study

Recipe #	Solvent	$TaCl_5$:$HfCl_4$:$C_{12}H_{22}O_{11}$:H_2O weight ratio	Expected Ta:Hf:C[a] molar ratio before CTR
R6	DI water	4.47:1:3.54:93.66	4:1:17
R7	DI water	1.11:1:1.35:19.70	1:1:6.50
R11	DI water	1.11:1:1.01:19.70	1:1:4.87
R13	DI water	4.47:1:2.65:93.66	4:1:12.75
		$TaCl_5$:$HfCl_4$:$(C_6H_6O{\cdot}CH_2O)_x$: 1-pentanol:ethanol weight ratio	
R10	1-pentanol & ethanol	1.11:1:2.18:197.16:81.57	1:1:6.50

[a]The carbon yield in pyrolysis at 700°C is considered as 18% for sucrose and 35% for phenolic resin, respectively, based on TGA results.

are aqueous-based, $TaCl_5$ and $HfCl_4$ were hydrolyzed separately in DI water giving fine white tantalum oxychloride ($TaOCl_3$) precipitate and colorless water-soluble hafnium oxychloride ($HfOCl_2$). The aqueous solution and suspension were mixed, and then sucrose was added. For recipe R10 that is organic solvent-based, $TaCl_5$ and $HfCl_4$ were dissolved together into 1-pentanol (99+%, Alfa Aesar # 30898) at room temperature forming a translucent solution, followed by the addition of phenolic resin, which was predissolved in a co-solvent of ethanol (99.5+%, Acros Organics #61509-0020) at concentration of 0.02 g/mL.

For all recipes, the obtained mixed solution/suspension was stirred continuously on a hot plate set at 300°C (the solution temperature was ~100°C) using a magnetic stir bar until they were completely dried. Then, the dried precursor's mixtures were pyrolyzed at 700°C for 1 hour in argon (UHP grade, Airgas) with a flow rate of 80 cc/min in a tube furnace with an inner diameter of 40 mm. During the pyrolysis process, precursors lose low molecular weight species (eg, water, carbon monoxide, and hydrogen chloride) to yield uniform amorphous (as shown later) Ta_2O_5-HfO_2-C fine mixtures. Most of the subsequent CTR heat treatments were performed isothermally in a tube furnace at 1500°C-1700°C for different holding times in flowing argon atmosphere. Due to the limited heating/cooling capability for the tube furnace used (up to 10°C/min), in some cases, a graphite rope was connected to a graphite boat containing the pyrolyzed powders and extended to the exhaust end of the tube furnace. The graphite rope was used to quickly pull the sample into and, later, out of the hot zone of the tube furnace preheated to CTR reaction temperature (eg, 1600°C) to investigate the effect of high heating/cooling rate (measured up to ~500°C/min) during the CTR process, as illustrated in the schematic in Figure S1A,B (see supplementary materials section (a)). In addition, to study the effect of electric field on the formation of $Ta_{0.5}Hf_{0.5}C$ solid solution/nanocomposite powders, CTR of the pyrolyzed powder from recipe R7 was also performed in a spark plasma sintering (SPS) system (Thermal Technologies, Model 10-4, Santa Rosa, CA, USA) under vacuum (base pressure of 2×10^{-2} torr) at 1600°C with a low applied pressure of 5 MPa in a 20 mm diameter graphite die set. To investigate the impact of the pressure alone on the phase formation/separation of $Ta_{0.5}Hf_{0.5}C$ powder, CTR of the R7 pyrolyzed powder was also carried out in the same SPS system but with two boron nitride (BN) disks touching the graphite die punches so that the BN disks would block the electric current from flowing through the sample (See Figure S1C in the supplementary materials section (a)). All pyrolyzed and CTR reaction products were characterized by X-ray diffraction (Siemens D5000) for phase identification. The morphology and particle size of the synthesized powders were studied by scanning electron microscope (SEM JEOL JSM-6330F) and transmission electron microscope (TEM Phillips CM-200). Thermogravimetric analysis (TGA) was carried out for some samples in the air with the constant heating rate of 10°C/min to determine the excess carbon content.

3 | RESULTS AND DISCUSSION

3.1 | Characterization of pyrolyzed material

Figure 1A,B show the XRD patterns of the samples from recipe R6 (Ta to Hf molar ratio of 4:1, or abbreviated as Ta:Hf=4:1 in this study) and R7 (Ta:Hf=1:1), respectively,

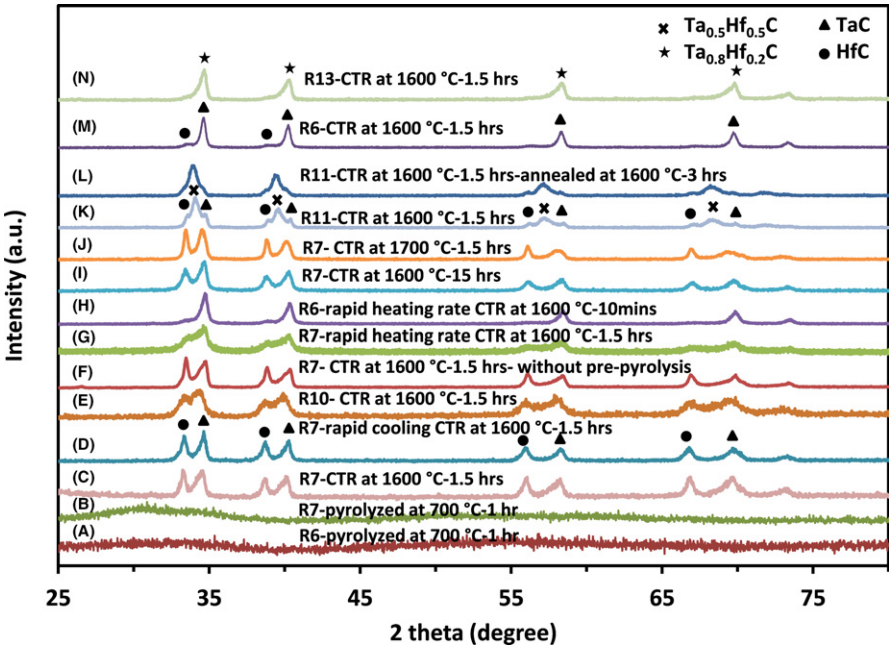

FIGURE 1 XRD patterns of synthesized powders for all recipes with different CTR conditions in a *tube furnace* [Color figure can be viewed at wileyonlinelibrary.com]

after pyrolysis at 700°C for 1 hour, indicating the formation of amorphous Ta and Hf oxides and carbon mixture after pyrolysis. This is favorable since crystallization of the Ta and Hf oxides might be accompanied by more segregation in oxides and negatively affects the homogeneity of the pyrolyzed material. The SEM image for the pyrolyzed powders gives an estimate for the particle size of ~50-100 μm with relatively dense structure (see Figure 2A for the sample from recipe R6).

3.2 | Observation of phase separation

To illustrate the possibility of forming phase-separated TaC-HfC nanocomposite powder, Figure 1C shows the XRD pattern for a sample from recipe R7 (Ta:Hf=1:1) synthesized via CTR at 1600°C for 1.5 hours. Instead of forming a uniform, single-phase $Ta_{0.5}Hf_{0.5}C$ solid solution powder, distinct peaks corresponding to individual HfC (JCPDS #98-008-5664) and TaC (JCPDS #98-008-5806) phases were observed for this sample. In addition, no other crystalline phases were identified by XRD. Figure 2B is the SEM image of this sample, showing the formation of relatively uniform nanosized (~50-100 nm) powder even though the sample is a composite of two individual carbide phase(s), as suggested by XRD.

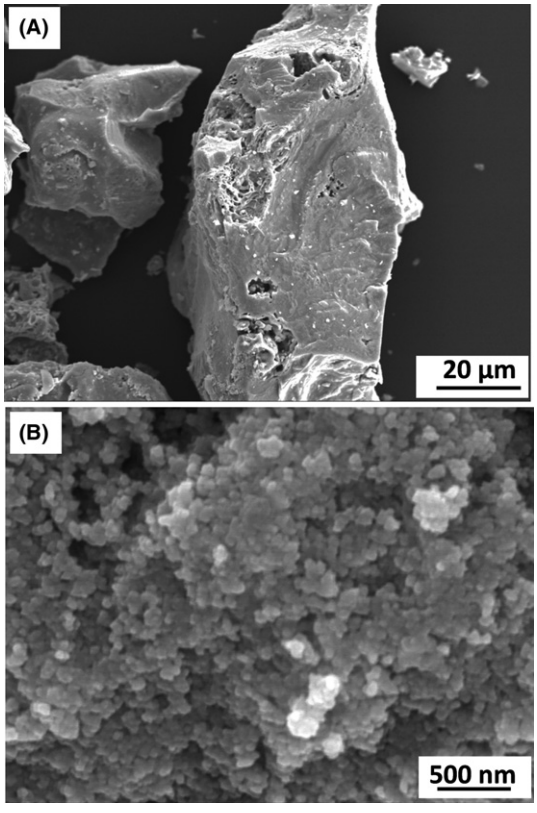

FIGURE 2 SEM micrographs of (A) pyrolyzed powders at 700°C for 1 h from recipe R6 (Ta:Hf=4:1) showing formation of 50-100 μm-sized particles with low porosity (B) synthesized powders via CTR at 1600°C for 1.5 h from recipe R7 (Ta:Hf=1:1) showing the formation of uniform nanosized powders (~<100 nm). It is noted that this sample is actually phase separated into TaC and HfC, as indicated by XRD (see Figure 1C)

3.3 | Understanding and controlling of phase separation

Upon carefully reviewing the TaC-HfC system, it is realized that there are several factors with respect to processing conditions and/or starting recipe that might contribute to the formation of separate TaC and HfC phases at CTR temperature of ~1600°C, which is well above the critical temperature of 887°C for the system. In the following, the results of a systematic study aimed at understanding the effects of those factors on controlling the phase(s) formed will be presented, and the implications of the experimental observations will also be discussed.

3.3.1 | Effect of CTR cooling rate

The first factor studied is cooling rate after the CTR heat treatment. This is because the CTR temperature of ~1600°C is well above the TaC-HfC system critical temperature. Therefore, it is possible that uniform solid solution powder could first form during CTR reaction. Then, upon slow cooling (eg, at ~10°C/min) inside the tube furnace, the uniform solid solution may go through phase separation (eg, via nucleation-growth or spinodal decomposition) and give a powder that becomes a two-phase mixture of TaC and HfC. To test such a hypothesis, a sample from recipe R7 (Ta:Hf=1:1) was synthesized via CTR at 1600°C for 1.5 hours, followed by rapid cooling. The fast cooling rate, estimated to be ~500°C/min, was realized by pulling the graphite sample boat directly out from the hot zone of the tube furnace to the cold zone (~80°C) after CTR at 1600°C for the designated time, as described in the experimental section. The expectation was that if the sample obtained using ~50 times faster cooling rate contains more solid solution comparing with the sample conventionally cooled at 10°C/min, it would support the hypothesis that $Ta_{1-x}Hf_xC$ solid solution forms first under the CTR condition and then goes through phase separation in the slow cooling stage.

Figure 1D shows the XRD pattern for this sample with rapid cooling after CTR: Individual TaC and HfC peaks are still clearly visible without any hint of solid solution formation. Comparing XRD for this sample with the sample cooled at the normal rate of 10°C/min (see Figure 1C), it is concluded that significantly faster cooling after CTR does not help prevent phase separation. The implication is that for the $Ta_{0.5}Hf_{0.5}C$ sample from recipe R7, only individual carbides are formed after CTR at 1600°C for

1.5 hours, while the expected $Ta_{0.5}Hf_{0.5}C$ single-phase solid solution has not been formed yet under this condition, probably due to the slow diffusion process, and the obtained nanopowder remains phase separated upon cooling to room temperature.

3.3.2 | Effects of solvent, prepyrolysis, and CTR heating rate

The second factor studied is related to solution processing. As mentioned in the introduction, uniform single-phase nanosized $Ta_{0.8}Hf_{0.2}C$ solid solution powders had been synthesized by other researchers via CTR using precursors obtained from organic solvent-based sol-gel or solvothermal processes.[10,14] In comparison, for this study, recipes such as R7 are water based. It was observed that upon addition of $TaCl_5$ to DI water, hydrolysis is very fast, leading to instantaneous precipitation of fine $TaOCl_3$ particles. On the other hand, $HfCl_4$ dissolves completely in water and forms a uniform and colorless solution. As a result, it is possible that the observation of separate TaC and HfC phases in the CTR product might have originated from the precipitation of $TaOCl_3$ upon fast $TaCl_5$ hydrolysis. This could lead to the loss of homogeneity of the liquid solution and cause large segregation of Ta-rich and Hf-rich regions persisting in subsequent steps of drying, pyrolysis, and finally CTR. Because of the large scale of separation caused by rapid $TaCl_5$ hydrolysis and precipitation, it would take a longer time for Ta and Hf to interdiffuse to obtain a uniform solid solution powder.

Thus, to test the hypothesis that a uniform liquid solution based on organic solvents, as adopted in other studies, would help reduce or even eliminate separation of Ta and Hf oxides in the solution processing (and later separation of carbides after CTR), less polar, organic solvent of 1-pentanol was used to reduce the rate of $TaCl_5$ hydrolysis, as described before for recipe R10 with the same Ta:Hf molar ratio of 1:1 as R7. This time, unlike when using water as the solvent, both $TaCl_5$ and $HfCl_4$ dissolve completely in 1-pentanol and form a uniform, translucent, light yellow-colored solution without any precipitation. However, the XRD pattern for the sample after CTR at 1600°C for 1.5 hours (Figure 1E) shows partially overlapping but still separated diffraction peaks corresponding to slightly Hf-doped TaC and Ta-doped HfC phases. Such an observation suggests the use of an organic solvent (and resulting slower hydrolysis) may help but is unlikely to be the critical factor to prevent phase separation of TaC and HfC for the final carbide products.

Similarly, the influence of removing the prepyrolysis step (ie, the 700°C/1 h heat treatment to convert the dried material from solution processing to intimate oxides-carbon mixture) and adoption of very fast heating rate (up to ~500°C/min) for CTR have also been explored for the same recipe R7. (Please refer to supplemental materials section (b) for detailed discussion of the rationale of studying these two factors), and their results are briefly summarized as in Figure 1F,G, respectively. Essentially, neither factor prevents the phase separation under the condition explored.

The observations that none of the factors discussed so far prevents the formation of separate TaC and HfC phases under the CTR condition explored (eg, 1600°C/1.5 hours) are attributed to the combined effect of several factors: First, there is very low affinity between the oxide precursors of Ta_2O_5 and HfO_2. To the best of the authors' knowledge, there is no binary phase diagram published for Ta_2O_5 and HfO_2. Nevertheless, the available phase diagram for the Ta_2O_5-ZrO_2[21] system shows that ZrO_2 has almost zero solubility of Ta_2O_5, whereas Ta_2O_5 can only accommodate ZrO_2 up to ~2 mol%. Due to the close chemical and physical similarity of Zr and Hf, it is reasonable to assume similar behavior for the Ta_2O_5-HfO_2 system, that is Ta_2O_5 and HfO_2 would have very low affinity for each other and do not form a solid solution with appreciable solubility.[22] The implication is that, despite the careful efforts in solution processing to mix Ta and Hf salts uniformly (eg, via the use of an organic solvent), the oxides of tantalum and hafnium, which can exist in amorphous form, will always segregate into separate Ta_2O_5 and HfO_2 regions. Second, the CTR reaction under the conditions explored is rather fast. One evidence for this claim is given in Figure 1H, which shows the XRD pattern for a sample from recipe R6 (Ta:Hf=4:1) synthesized via rapid heating CTR at 1600°C for a short time of only 10 minutes: Both TaC and HfC formed individually after only 10 minutes of CTR without any trace of remaining oxides at that temperature. (Note Figures like 1H have been shrunk vertically for plotting purpose, which makes minor peaks corresponding to HfC less visible.) The combined effect of those two factors mentioned above is that the segregated (amorphous) Ta_2O_5 and HfO_2 regions will always go through separate CTR reactions to form TaC and HfC phases. Then rely on interdiffusion of Ta and Hf in the high-temperature carbide phases to form a uniform, single-phase solid solution ternary carbide. On the other hand, the interdiffusion of Ta and Hf at these temperatures can be slow,[23] which explains why separate TaC and HfC remain even though the CTR temperature is significantly above the miscibility gap.

3.3.3 | Effects of CTR temperature and holding time

As explained above, due to the low affinity between Ta_2O_5 and HfO_2 and the large difference in driving force for the formation of TaC and HfC (see supplementary materials

section (b)), the two carbides would always form individually in CTR; then the solid solution forms via interdiffusion between them, which can take a significant time. As a result, the formation of $Ta_xHf_{1-x}C$ single-phase solid solution is expected to improve when using higher CTR temperatures and/or longer CTR dwell times. Indeed, Figure 3A shows the XRD patterns (showing a zoomed section) for a sample from the Ta-rich recipe R6 (Ta:Hf=4:1) after CTR at 1500°C for 3 hours and the same sample after additional annealing at 1600°C for 10 hours in argon. The as-synthesized sample after CTR at 1500°C for 3 hours shows clear separation of TaC and HfC phases, while after the additional annealing at 1600°C for 10 hours, the individual TaC and HfC diffraction peaks merged completely to ones that correspond to a uniform, single-phase solid solution of $Ta_{0.8}Hf_{0.2}C$.

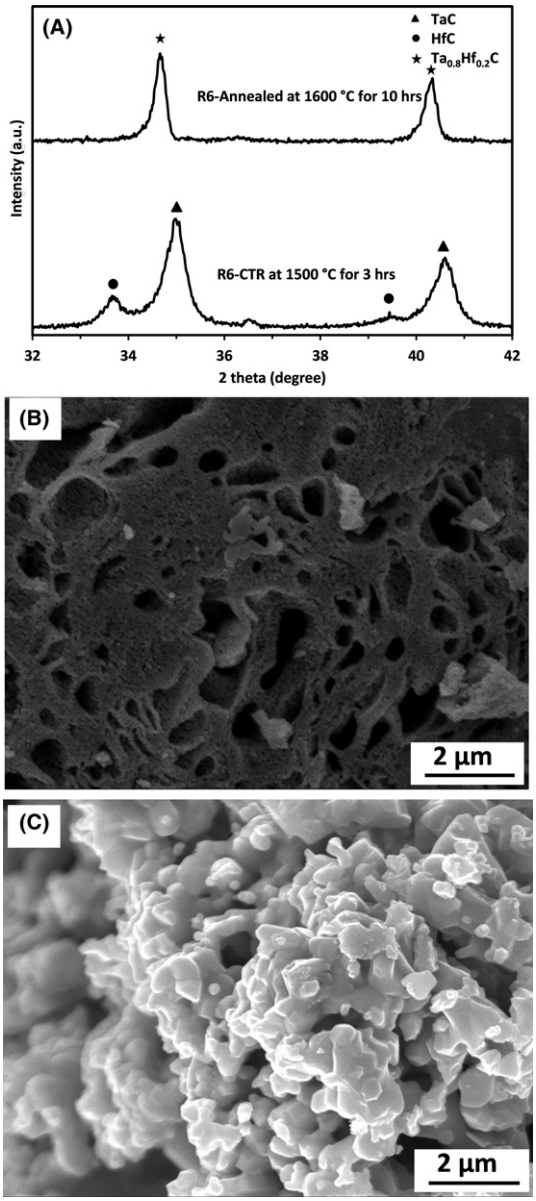

FIGURE 3 (A) XRD pattern for the sample from recipe R6 (Ta:Hf=4:1) synthesized via CTR at 1500°C, annealed for 10 h at 1600°C (B) SEM image of this sample before annealing showing the formation of uniform nanosized powders (C) after annealing at 1600°C for 10 h indicating a noticeable grain growth

However, it is noted that there are limitations on the use of higher CTR temperature or very long CTR dwell time to help the formation of a single-phase solid solution powders. First, they would lead to excessive grain growth, which is undesirable for the purpose of synthesizing nanosized solid solution powders. Figure 3B shows the SEM images of the sample from recipe R6 obtained from CTR at 1500°C for 3 hours, whereas Figure 3C is for the same sample after additional annealing at 1600°C for 10 hours to convert the two-phase composite powder into a single-phase solid solution powder. All particles experience significant coarsening with primary grain size increased from ~50 nm to up to ~500 nm. Second, higher temperature or longer time would add to energy consumption and process cost. Last but not least, for the certain compositions, it may not be effective: Take the example of a Hf-richer sample from recipe R7 (Ta:Hf=1:1), even 15 hours of CTR at 1600°C or higher CTR temperature of 1700°C did not seem to prevent the phase separation of TaC and HfC, as shown in Figure 1I,J, respectively.

3.3.4 | Effect of excess (amorphous) carbon content

The seeming difficulty in obtaining single-phase $Ta_xHf_{1-x}C$ nano solid solution powders prompts additional analysis of the various samples obtained. Figure 4A,B are the TEM images for the sample from recipe R7 (Ta:Hf=1:1) synthesized via CTR at 1600°C for 1.5 hours. The images confirm the synthesized TaC-HfC composite powders are nanograined with a primary particle size of ~50 nm, which is consistent with SEM observation (see Figure 2B). In addition, the images also suggest that each of the nanocarbide particles seems to have a low-atomic mass shell over it. (High-resolution TEM and EDS will be needed to characterize the solid solution nanopowders further.) In addition, TGA analysis of this sample in air, as shown in Figure 5A, indicates that the sample has carbon excess of ~9.5 wt%. Because XRD pattern for that sample (see Figure 1C) did not show the presence of any crystalline carbon, carbon must exist in amorphous form, and it is likely that the observed amorphous shell is amorphous carbon on the surface of individual TaC/HfC nanoparticles.

Considering that (i) Ta_2O_5-HfO_2 immiscibility and fast CTR kinetics lead to the formation of individual TaC and HfC phases and (ii) excessive (amorphous) carbon might exist as shells over those individual carbide nanoparticles, the effect of excess carbon content (or starting

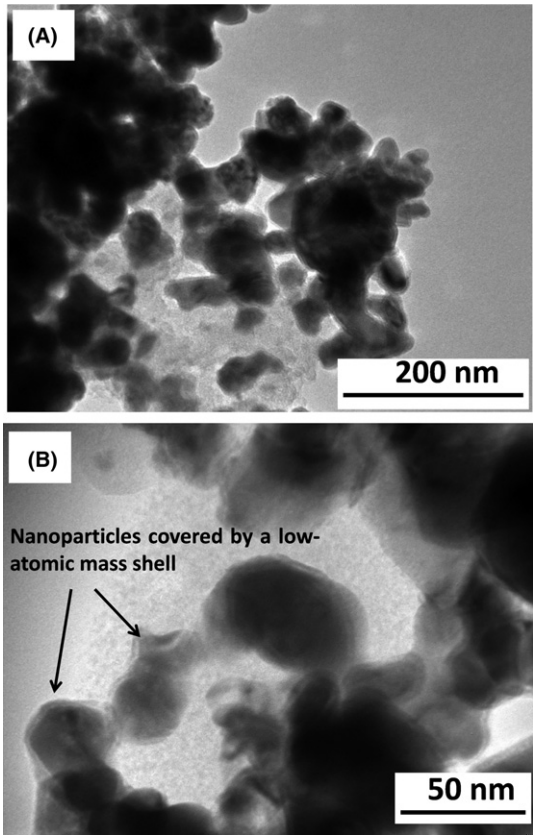

FIGURE 4 TEM images of TaC-HfC nanocomposite powders synthesized via CTR at 1600°C for 1.5 h from recipe R7 (Ta:Hf=1:1) showing the formation of nanosized particles (~<50 nm) often covered by a low-atomic mass shell that is assumed to be amorphous carbon

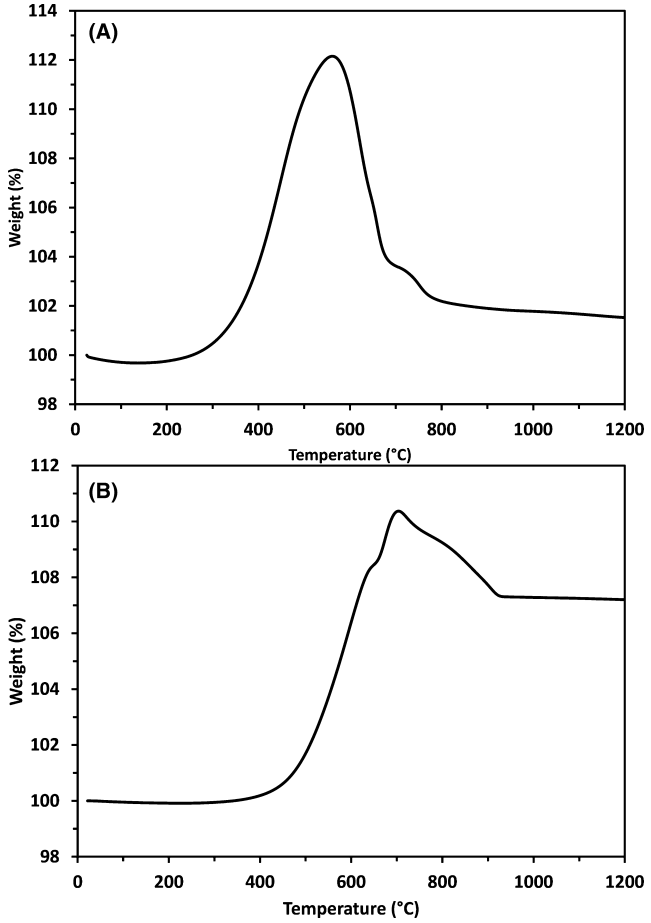

FIGURE 5 TGA analysis in air of synthesized powders at 1600°C via CTR in the tube furnace from aqueous recipes of (A) R7 (Ta:Hf:C=1:1:6.5 before CTR) and (B) R11 (Ta:Hf:C=1:1:4.87 before CTR)

composition) on phase separation of TaC and HfC in the synthesis was investigated. The hypothesis was that the excess carbon in the form of (amorphous) carbon shell over the individual carbide phases might dramatically inhibit the interdiffusion of Ta and Hf cations between HfC and TaC grains and, as a result, slow the solid solution formation. To test this hypothesis, a sample from recipe R11 with lower carbon content than recipe R7 but the same Ta:Hf molar ratio of 1:1 was synthesized via solution processing and subsequent CTR at 1600°C for 1.5 hours. Figure 1K gives the XRD pattern for this sample: Individual peaks corresponding to phase-separated HfC and TaC along with $Ta_{0.5}Hf_{0.5}C$ solid solution peaks in between, as expected from Vegard's law, were all detected. TGA for this sample indicates it indeed has a lower excess carbon content of ~4.6 wt%, consistent with the lower carbon recipe R11 used (see Figure 5B). Therefore, it is evident that lower excess carbon content dramatically improves the interdiffusion and the formation of a solid solution. Further annealing of this sample for an additional 3 hours enhances the solid solution formation noticeably with the individual carbide peaks almost disappearing, as shown in Figure 1L. In comparison, as mentioned before for Figure 1I, for a sample from recipe of R7 (Ta:Hf=1:1) with higher starting sucrose content, CTR for 15 hours at 1600°C did not give the same effect in promoting the formation of a uniform solid solution phase.

These results suggest that excess carbon content seems to play a dominating role in determining the phase separation in $Ta_xHf_{1-x}C$ synthesis via CTR reaction: Excess carbon would slow down the interdiffusion dramatically and greatly inhibit the solid solution formation leading to the formation of individual TaC and HfC phases. The excess carbon effect may also help explain the variations between observations made in this study and those reported in the literature. For example, Jiang et al.[14] reported the formation of single-phase $Ta_{0.8}Hf_{0.2}C$ solid solution powder after 1600°C/1 hour CTR, whereas in this study, when using recipe R6 with the same target Ta:Hf molar ratio, minor peaks corresponding to HfC were observed (see Figure 1M). To further confirm this explanation, experiments using an aqueous-based recipe R13 (Ta:Hf=4:1) with

reduced carbon content were carried out. For this sample, the peaks corresponding to HfC were disappeared and merged with TaC peaks (see Figure 1N). However, it should be noted that the observed peaks in Figure 1N do not have the symmetric shape. This nonsymmetric distribution in the peak profile can be due to the chemical variation such as inhomogeneity of the solid solution. The lattice parameter (a) for this sample was calculated to be ~0.4486 nm using the peaks positions in Figure 1N, which is close to $Ta_{0.8}Hf_{0.2}C$ solid solution lattice parameter as expected from the Vegard's law and the reported JCPDS card (a=0.4487 nm, # 00-064-0146).

Hence, it is advised that in future synthesis great attention should be given to precisely control and optimize carbon precursor content in starting materials for the synthesis of $Ta_xHf_{1-x}C$ powders: A significant amount of excess carbon would make the uniform solid solution phase difficult to obtain, whereas too low carbon content might risk incomplete CTR and excessive oxide remaining in the product. It is also noted that the observation concerning the dramatic influence of excess carbon on Ta and Hf cation interdiffusion may also throw light into understanding the large variation in sintering kinetics observed for TaC-HfC materials.

3.3.5 | Effect of DC electric field and applied pressure

Finally, as stated, the authors also performed CTR using pyrolyzed powders from recipe R7 (Ta:Hf=1:1) in an SPS instrument at 1600°C for 15 minutes with a low applied pressure of 5 MPa. The purpose was to find out the effect of the external electrical field on the phase formation/separation for $Ta_xHf_{1-x}C$ nanopowder materials, and it was inspired by the reported advantages of applying electric field and pressure in SPS on accelerating mass transport and sintering kinetics for ceramic materials.[15,18,24,25] The SPS temperature, time, and pressure were all intentionally kept at the low end to avoid excessive sintering/grain growth since the goal was to synthesize $Ta_xHf_{1-x}C$ nanopowders and not to sinter the powders into a dense ceramic body. Figure 6A shows the XRD pattern for this sample. The diffraction peaks corresponding to individual TaC and HfC phases disappeared completely, whereas the peaks corresponding to the single-phase $Ta_{0.5}Hf_{0.5}C$ solid solution (matching JCPDS card #98-005-4915 and the expectation from Vegard's law) were observed. The SEM image of this sample shows the formation of fine uniform powder with a grain size of ~100 nm (see Figure 7A). EDS analysis confirmed the Ta:Hf atomic ratio of 1 to 1, while carbon to total metal (Ta plus Hf) atomic ratio is much higher than 1 to 1, which is consistent with the TGA result for other samples from recipe R7 (see Figure 5A). In

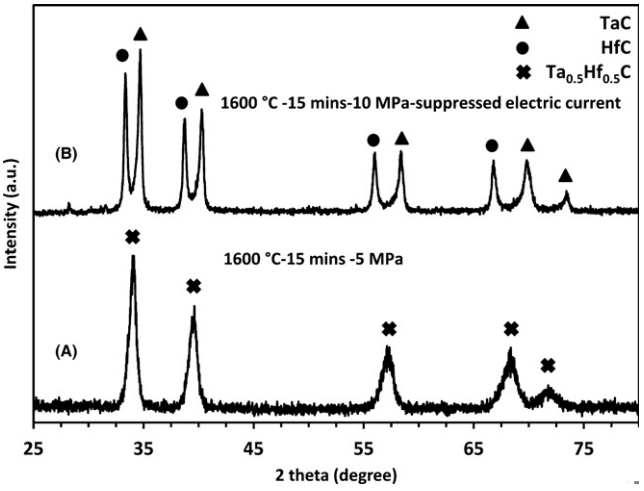

FIGURE 6 XRD patterns of synthesized powders from aqueous recipe R7 (Ta:Hf=1:1) via CTR in the SPS instrument at 1600°C for 15 minutes: (A) under pressure of 5 MPa with current passing through the sample, (B) under pressure of 10 MPa, while the electric current passing through the sample was suppressed using BN disks as insulator

comparison, when SPS was carried out at the same temperature of 1600°C but only for 1 minute, the XRD pattern shows the formation of clearly phase separated TaC and HfC without the detectable amount of either carbide solid solution or oxides. The results from these two experiments suggest that the condition provided by SPS greatly accelerates the interdiffusion between TaC and HfC and promotes the formation of single-phase $Ta_xHf_{1-x}C$ solid solution; only ~15 minutes of isothermal hold is required to achieve the transformation from individual carbides to the solid solution phase, and the solid solution phase would remain upon cooling to room temperature.

To confirm if the above observation of accelerated solid solution formation in SPS using sample from recipe R7 is due to the electric field alone and not the low pressure (5 MPa) applied in SPS, another experiment was performed in the SPS at the same temperature of 1600°C for the same time of 15 minutes under an even higher pressure of 10 MPa. As described before in the experimental section, for this time, the pyrolyzed powders, instead of touching the graphite die punches directly, were sandwiched between two insulating BN disks (see Figure S1C in the supplementary materials section (a).) so that almost no DC electrical current would pass through the sample. The XRD pattern for this sample is given in Figure 6B. Diffraction peaks corresponding to individual TaC and HfC were clearly observed with no hint of any solid solution formation. Hence, it is concluded that the applied pressure (5-10 MPa) does not play a major role in forming of single-phase $Ta_{0.5}Hf_{0.5}C$ solid solution powder, and it is the applied DC electrical field that helps the interdiffusion

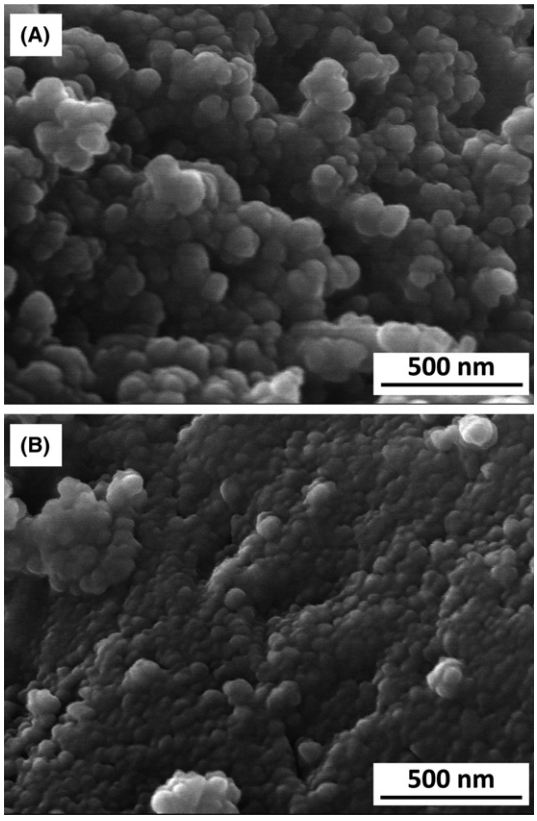

FIGURE 7 SEM micrographs of synthesized powders from recipe R7 (Ta:Hf=1:1) via CTR in the SPS instrument at 1600°C for 15 min: (A) under pressure of 5 MPa with electric current passing through the sample, (B) under pressure of 10 MPa, while electric current passing through the sample was suppressed using BN disks as insulator. Note that both samples consist of uniform fine powders. However, coarsening due to the electric current passing through the sample is noticeable for (A)

between TaC and HfC and accelerates the solid solution formation process. Simple estimation shows that the Ta^{+4}/Hf^{+4} migration length due to the DC electrical field at 1600°C for 15 minutes (as used for the CTR via SPS experiment) would be only on the order of ~1 nm, which is much shorter than the particle radius. (The readers could refer to supplemental materials section (c) for details of the estimation.) Such an analysis suggests that the acceleration of $Ta_{0.5}Hf_{0.5}C$ solid solution formation from individual TaC and HfC carbide phases in as short as 15 minutes when using SPS could not be due to the drift effect. Therefore, it is hypothesized that high concentration of vacancies are created under the high current/high flux condition of SPS, which speeds up the diffusion of cations.

However, it should be noted that, while applied DC electrical field accelerates the mass transport and faster interdiffusion and facilitate faster formation of uniform solid solution, it has limitation in that the applied DC electrical field also leads to more coarsening of the particles. As shown from the SEM image for the sample synthesized via CTR in SPS at 1600°C for 15 minutes under the pressure of 5 MPa (see Figure 7A): the grain size for the powder is ~100 nm, which is significantly larger than both the sample obtained with BN disks suppressing the electric current during SPS (see Figure 7B) showing grain size of only ~50 nm and the conventional 1600°C/1.5 hours CTR sample showing grain size of 50 nm (see for example Figure 3B). The obtained result is also consistent with earlier reports that SPS greatly accelerated the sintering for UHTC such as TaC and HfC compared with conventional sintering.[15,18,24,25]

4 | CONCLUSIONS

In this work, the synthesis of the nanocrystalline $Ta_{1-x}Hf_xC$ solid solution and related nanocomposite powders was achieved using aqueous solution-based processing from low-cost $TaCl_5$, $HfCl_4$, and carbon sources of sucrose followed by pyrolysis and CTR. Phase separation of TaC and HfC was observed for Hf-richer samples of $Ta_{0.5}Hf_{0.5}C$ regardless of varying processing parameters such as CTR reaction temperature, holding time, and cooling/heating rates as well as solvent type. The strong tendency for forming phase-separated TaC-HfC nanopowders composites instead of uniform solid solution powders is attributed to the difference in reactivity between oxides of Ta_2O_5 and HfO_2 and carbon, which is also related to the immiscibility of those two oxides. Such a difference always leads to the formation of individual TaC and HfC nanopowders even after a relatively short CTR time (eg, 10 minutes at 1600°C). On the other hand, it was discovered that reducing the excess carbon content or the application of a DC electrical field (as through the use of SPS) would significantly accelerate the diffusion and help the formation of single-phase $Ta_{0.5}Hf_{0.5}C$ solid solution powders. (Readers may also refer to Table S1 in the supplementary materials section (d) for a summary of experimental observation and their implications.) This study illustrates the complexity of the composition-processing-structure relationship during synthesis of multicomponent UHTC nanomaterials. The knowledge generated about how to understand and control phase separation during the synthesis of nanosized $Ta_xHf_{1-x}C$ single-phase solid solution versus two-phase composite powders would enhance understanding of other related phenomena as encountered in sintering of these materials as well as the synthesis of other related multicomponent UHTC materials.

ACKNOWLEDGMENTS

The authors thank Dr. Shravana Katakam at FIU AMERI for taking the TEM images.

REFERENCES

1. Cheng Z, Foroughi P, Behrens A. Synthesis of nanocrystalline TaC powders via single-step high temperature spray pyrolysis from solution precursors. *Ceram Int*. 2016;42:8-11.
2. Savino R, De Stefano Fumo M, Paterna D, et al. Arc-jet testing of ultra-high-temperature-ceramics. *Aerosp Sci Technol*. 2010;14:178-187.
3. Levine SR, Opila EJ, Halbig MC, et al. Evaluation of ultra-high temperature ceramics for aeropropulsion use. *J Eur Ceram Soc*. 2002;22:2757-2767.
4. Opeka MM, Talmy IG, Wuchina EJ, et al. Mechanical, thermal, and oxidation properties of refractory hafnium and zirconium compounds. *J Eur Ceram Soc*. 1999;19:2405-2414.
5. Wuchina E, Opeka M, Causey S, et al. Designing for ultrahigh-temperature applications: the mechanical and thermal properties of HfB2, HfCx, HfNx and αHf(N). *J Mater Sci*. 2004;39:5939-5949.
6. Bellosi A, Monteverde F. Ultra-high temperature ceramics: microstructure control and properties improvement related to materials design and processing procedures. *Euro Space Agency* 2006;631:46.
7. Ghaffari SA, Faghihi-Sani MA, Golestani-Fard F, et al. Pressureless sintering of $Ta_{0.8}Hf_{0.2}C$ UHTC in the presence of $MoSi_2$. *Ceram Int*. 2013;39:1985-1989.
8. Arianpour F, Golestanifard F, Rezaie H, et al. Processing, phase evaluation and mechanical properties of $MoSi_2$ doped 4TaC–HfC based UHTCs consolidated by spark plasma sintering. *Int J Refract Met Hard Mater*. 2016;56:1-7.
9. Andrievskii RA, Strel'nikova NS, Poltoratskii NI, et al. Melting point in systems ZrC–HfC, TaC–ZrC, TaC–HfC. *Poroshk. Metall.* 1967;1:85-88.
10. Simonenko EP, Ignatov NA, Simonenko NP, et al. Synthesis of highly dispersed super-refractory tantalum-zirconium carbide Ta_4ZrC_5 and tantalum–hafnium carbide Ta_4HfC_5 via Sol-gel technology. *Russ J Inorg Chem*. 2011;56:1681-1687.
11. Foroughi P, Cheng Z. Understanding the morphological variation in the formation of B_4C via carbothermal reduction reaction. *Ceram Int*. 2016;42:15189-15198.
12. Wollmershauser JA, Feigelson BN, Gorzkowski EP, et al. An extended hardness limit in bulk nanoceramics. *Acta Mater*. 2014;69:9-16.
13. Gaballa O, Cook BA, Russell AM. Reduced-temperature processing and consolidation of ultra-refractory Ta_4HfC_5. *Int J Refract Met Hard Mater*. 2013;41:293-299.
14. Jiang J, Wang S, Li W. Preparation and characterization of ultra-high-temperature ternary ceramics Ta_4HfC_5. *J Am Ceram Soc*. 2016;4:1-4.
15. Cedillos-Barraza O, Grasso S, Al Nasiri N, et al. Sintering behaviour, solid solution formation and characterisation of TaC, HfC and TaC–HfC fabricated by spark plasma sintering. *J Eur Ceram Soc*. 2016;36:1539-1548.
16. Zhang C. High temperature oxidation study of tantalum carbide-hafnium carbide solid solutions synthesized by spark plasma sintering. Ph.D. Thesis. Florida International University, Florida. 2016.
17. Gaballa OG. Processing development of 4TaC–HfC and related carbides and borides for extreme environments. Ph.D. Thesis. Iowa State University, Iowa. 2012.
18. Zhang C, Gupta A, Seal S, et al. Solid solution synthesis of tantalum carbide-hafnium carbide by spark plasma sintering. *J Am Ceram Soc*. 2017;100:1853-1862.
19. Adjaoud O, Steinle-Neumann G, Burton BP, et al. First-principles phase diagram calculations for the HfC–TiC, ZrC–TiC, and HfC–ZrC solid solutions. *Phys Rev B – Condens Matter Mater Phys* 2009;80:32-34.
20. Schönfeld B, Engelke M, Ruban AV. Lack of support for adaptive superstructure NiPt7: experiment and first-principles calculations. *Phys Rev B – Condens Matter Mater Phys* 2009;79:1-12.
21. Bhattacharya AK, Shklover V, Steurer W, et al. Ta_2O_5–Y_2O_3–ZrO_2 system: experimental study and preliminary thermodynamic description. *J Eur Ceram Soc*. 2011;31:249-257.
22. Li GD, Wu M, Xiong X, et al. Preparation and ablation properties of Hf(Ta)C co-deposition coating for carbon/carbon composites. *Corros Sci*. 2013;66:177-182.
23. Ghaffari SA, Faghihi-Sani MA, Golestani-Fard F, et al. Diffusion and solid solution formation between the binary carbides of TaC, HfC and ZrC. *Int J Refract Met Hard Mater*. 2013;41:180-184.
24. Ghaffari SA, Faghihi-Sani MA, Golestani-Fard F, et al. Spark plasma sintering of TaC–HfC UHTC via disilicides sintering aids. *J Eur Ceram Soc*. 2013;33:1479-1484.
25. Munir ZA, Anselmi-Tamburini U, Ohyanagi M. The effect of electric field and pressure on the synthesis and consolidation of materials: a review of the spark plasma sintering method. *J Mater Sci*. 2006;41:763-777.

SUPPORTING INFORMATION

Additional Supporting Information may be found online in the supporting information tab for this article.

How to cite this article: Foroughi P, Zhang C, Agarwal A, Cheng Z. Controlling phase separation of $Ta_xHf_{1-x}C$ solid solution nanopowders during carbothermal reduction synthesis. *J Am Ceram Soc*. 2017;100:5056–5065. https://doi.org/10.1111/jace.15065